Journal of the European Ceramic Society 22 (2002) 2001–2012

www.elsevier.com/locate/jeurceramsoc

Charge and mass transport in ceramic TiO_2

Marta Radecka[a], Mieczyslaw Rekas[b,*]

[a]*Faculty of Materials Science and Ceramics, University of Mining and Metallurgy, 30-059 Krakow, Poland*
[b]*School of Materials Science and Engineering, The University of New South Wales, Sydney, NSW 2052, Australia*

Received 8 June 2001; received in revised form 14 November 2001; accepted 8 December 2001

Abstract

This paper is a report on the electrical conductivity properties of ceramic TiO_2 materials sintered at different temperatures within the range of 1200–1400 °C (1473–1673 K). The measurements were taken in the temperature range 650–1080 °C (923–1353 K) and oxygen partial pressure, $p(O_2)$, 10–10^5 Pa. The determined values of the $p(O_2)$ exponent differ from those predicted by defect disorder models. This difference allows us to evaluate both electronic and ionic components of the electrical conductivity. Using the Nerst–Einstein equation, the determined ionic component was verified against diffusion data in available literature. The energy gap was determined from both optical and electrical studies. © 2002 Published by Elsevier Science Ltd.

Keywords: Diffusion; Electrical conductivity; Energy band gap; TiO_2

1. Introduction

The electrical properties of reduced titanium dioxide are the subject of numerous works due to its technical importance as an electronic material (for capacitors, varistors etc.).[1–7] Much less is known about the properties of titanium dioxide equilibrated in oxygen-rich atmospheres, where p-type conductivity is observed.

The defect structure and related properties of TiO_2 are usually deduced from electrical conductivity measurements, assuming that the studied material is an electronic semiconductor. According to our previous studies,[8–10] this assumption seems to be valid in the case of strongly reduced or donor-doped rutile. However, for undoped material within the p-type range and in the $p(O_2)$ range close to the n–p transition point, this assumption is not reliable.[10]

Studies of the defect structure and related electrical properties of semiconducting materials are more often performed on polycrystalline materials than on single crystals. This happens because either the single crystals are not available or our interest is directed towards polycrystalline materials due to their technical importance. The presence of grain boundaries in polycrystalline samples may cause the semiconducting and transport properties to differ substantially with respect to single-crystalline materials. Despite a number of research works devoted to polycrystalline materials, there are still many unresolved problems concerning the impact of biography; mainly the sintering conditions, as well as the effect of micro-structure on studied properties. The incomplete studies performed on this material postulated that ionic conductivity of oxide materials is enhanced by the presence of grain boundaries.[11] The aim of this paper is to provide a systematic study of the effect of sintering conditions on charge and mass transport in ceramic TiO_2 materials and comparison of the obtained results with the results reported for single crystal TiO_2.[10]

2. Experimental

TiO_2 specimens were prepared by precipitation of hydroxides from aqueous solutions of $TiCl_4$, using ammonia. The details concerning sample preparation are described elsewhere.[12] Specimens that were sintered in air for 5 h at 1200, 1300 and 1400 °C (1473, 1573 and 1673 K) are the subject of these studies. The electron microscopy observations revealed that the specimens exhibit grain sizes between 2–3, 6–8 and 40–100 μm for the sintering temperatures 1200, 1300 and 1400 °C (1473, 1573 and 1673 K), respectively. The D.C. conductivity

* Corresponding author. Tel.: +61-2-9385-6459; fax: +61-2-9385-6467.
E-mail address: m.rekas@unsw.edu.au (M. Rekas).

0955-2219/02/$ - see front matter © 2002 Published by Elsevier Science Ltd.
PII: S0955-2219(01)00519-2

was determined using the four-probe method within the temperature range 650–1080 °C (923–1353 K). The experimental procedure involved the determination of electrical conductivity of the TiO_2 specimens, achieving equilibrium by making changes in $p(O_2)$ in the gas phase, while keeping the temperature constant. The measurements of electrical conductivity were performed within the $p(O_2)$ range, where the expected[9] electronic conductivity obeys the law $\sigma \sim p(O_2)^{\pm 1/4}$. The required $p(O_2)$ was imposed using an argon/oxygen mixture flowing at a rate of 100 cm^3/min over the TiO_2 specimen, and then monitoring the changes in electrical conductivity against time. It is assumed that equilibrium between samples and the surrounding gas atmosphere is established when electrical conductivity has reached a constant value. The equilibration time was approximately 30 min. This time involves both the time required to achieve a constant value of $p(O_2)$ and the real time needed for vanishing of the nonstoichiometry gradient between the surface and the bulk of crystals through the mass transport.

Fundamental optical transitions from the valence to the conduction band at room temperature were studied by optical methods. A Lambda 19 Perkin Elmer double beam spectrophotometer was used to measure the spectral dependence of diffused reflectance $R_{Diff}(\lambda)$ over the wide wavelength range of $\lambda = 200$–2500 nm. Light scattering experiments were carried out with a 150-mm integrating sphere (IS). Diffused reflectance was measured with the light trap in the specularly reflected beam.

3. Results

Figs. 1–3 illustrate changes in the electrical conductivity coefficient as a function of $p(O_2)$ of the TiO_2 samples, sintered at 1200, 1300 and 1400 °C (1473, 1573

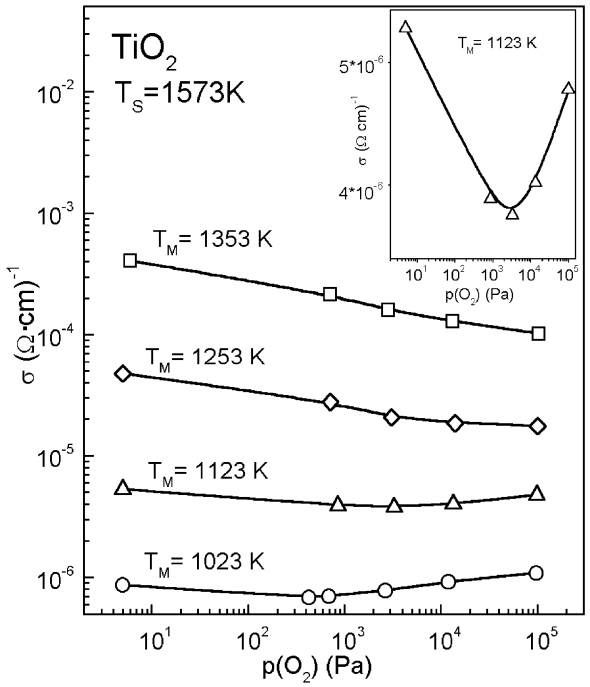

Fig. 2. Electrical conductivity as a function of $p(O_2)$ for TiO_2 sintered at 1300 °C (1573 K) in air for 5 h.

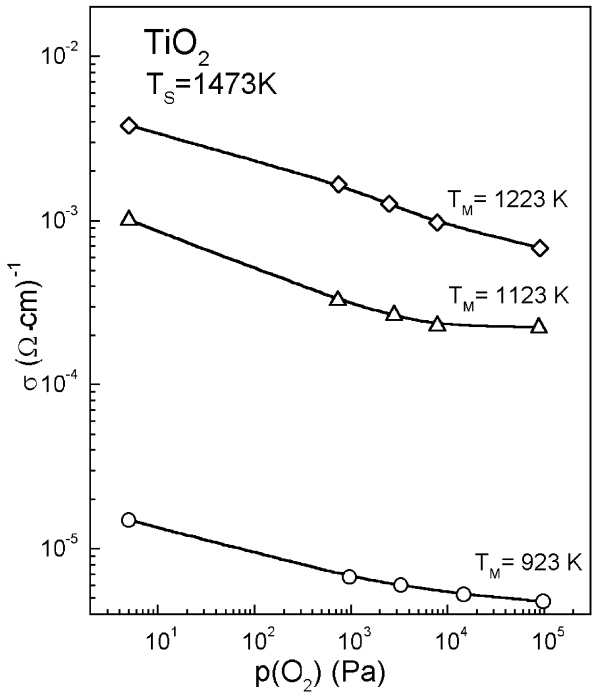

Fig. 1. Electrical conductivity as a function of $p(O_2)$ for TiO_2 sintered at 1200 °C (1473 K) in air for 5 h.

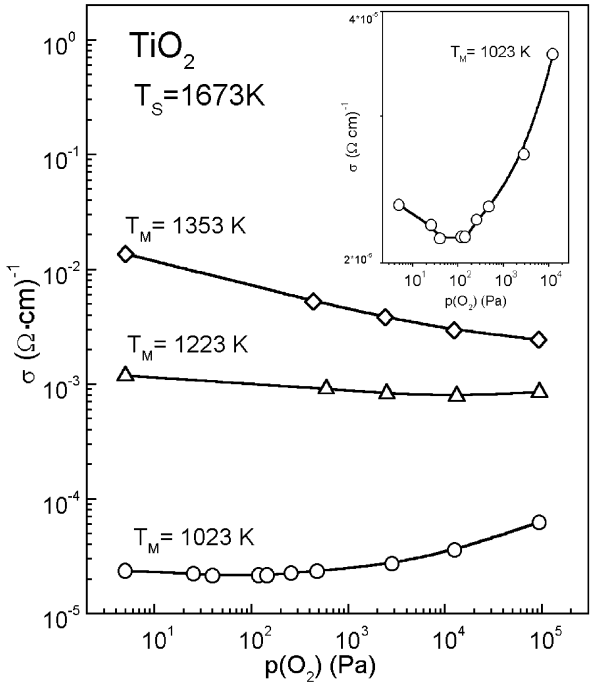

Fig. 3. Electrical conductivity as a function of $p(O_2)$ for TiO_2 sintered at 1400 °C (1673 K) in air for 5 h.

and 1673 K), respectively. Some of the presented dependencies exhibit a minimum value of σ ($T_S = 1573$ K and $T_M = 1123$ and 1023 K; $T_S = 1673$ K and $T_M = 1023$ K and $T_M = 1223$ K). The minimum values of σ are shown in more detail on the insets in Figs. 2 and 3. The existence of a minimum value of σ indicates the n- to p- type transition. The effect of the sintering temperature on the n–p transition in TiO_2 is described elsewhere.[12]

4. Discussion

4.1. Determination of ionic conductivity

As mentioned above, the density of grain boundaries may affect ionic transport numbers in ceramic material. The electrical conductivity σ_{total}, may by expressed as a sum:

$$\sigma_{total} = \sigma_n + \sigma_p + \sigma_{ion} = \sigma_{el} + \sigma_{ion} = e(n\mu_n + p\mu_p) + \sigma_{ion} \quad (1)$$

where subscripts n, p, el and ion correspond to electron, electron hole, electronic and ionic components of conductivity, respectively.

According to defect chemistry,[9,10] in the region close to the n–p transition, the electron and electron hole electrical conductivity components are always (whichever defect model is used) expressed in terms of the following function of $p(O_2)$:

$$\sigma_n = \sigma_n^o p(O_2)^{-1/4} \quad (2)$$

$$\sigma_p = \sigma_p^o p(O_2)^{1/4} \quad (3)$$

On the other hand, the ionic component σ_{ion} remains independent of $p(O_2)$.

Taking into considerations Eqs. (2) and (3), Eq. (1) assumes the form:

$$\sigma = \sigma_n + \sigma_p + \sigma_{ion} = \sigma_n^o p(O_2)^{-1/4} + \sigma_p^o p(O_2)^{1/4} + \sigma_{ion}^o \quad (4)$$

where the superscript "o" indicates that the term is independent of oxygen activity.

The separation of both ionic and electronic components from the total electrical conductivity is usually done by analysing the dependence (4) separately within either n- or p- type regions.[13] In the n- type range it is assumed that σ_p is negligible small (especially $\sigma_{ion} \gg \sigma_p$), thus the dependence (4) assumes the form:

$$\sigma_{total} = \sigma_n + \sigma_{ion} = \sigma_n^o p(O_2)^{-1/4} + \sigma_{ion}^o \quad (5)$$

Analogously, in the p-type region $\sigma_{ion} \gg \sigma_n$. Then we have:

$$\sigma_{total} = \sigma_p + \sigma_{ion} = \sigma_p^o p(O_2)^{1/4} + \sigma_{ion}^o \quad (6)$$

Eqs. (5) and (6) indicate, that σ_{total} plotted vs. $p(O_2)^{-1/4}$ or $p(O_2)^{1/4}$ in the n and p-type regions, respectively, give straight lines with the intersect corresponding to the σ_{ion}^o .This procedure was successfully used to determination both ionic and electronic components of electrical conductivity in case ThO_2,[14–17] ZrO_2,[18,19] Bi_2O_3,[20] $LaAlO_3$,[21] CeO_2[22,23] and alkaline metal earth titanates.[13]

However, in case of TiO_2 this procedure may have failed because of a narrow range of $p(O_2)$ where dependence (4) is valid. Namely, at low $p(O_2)$ (n-type region) this range is limited by experimentally observed change of the electroneutrality condition and the resulting change of the parameter m_σ [precise definition of m_σ is done below by Eq. (9)] from $m_\sigma = -4$ to $m_\sigma = -6$ (when doubly ionized oxygen vacancies, $V_{\ddot{O}}$, predominate) or to $m_\sigma = -5$ (when titanium interstitial, Ti_i^{4+}, is a predominant defect). On the other hand, at high $p(O_2)$ the required range is limited by $p(O_2) = 0.1$ MPa (1 atm) due to technical conditions of experiment (the electrical properties of oxide materials are commonly studied below $p(O_2) = 1$ atm, only few experiments are repotted above this value[24–26]). The described limitations for TiO_2 cause that the approximations (5) and (6) cannot be used due to the lack of available experimental points corresponding to either pure n- or p- type conductivity. Fig. 4 schematically illustrates the dependence (2)–(4) for arbitrary chosen parameters $\sigma_n^o = \sigma_p^o = 1$ and $\sigma_{ion} = 0$ (curve $\sigma_n + \sigma_p$) and $\sigma_{ion} = 2$ (curve σ_{total}). The parameter n_σ at low $p(O_2)$ (below 10^{-4} Pa) was assumed equal to -5.5. According to Fig. 4, there are three $p(O_2)$ regions of $p(O_2)$:

(1) n-type, where the approximation (5) may be applied,
(2) p-type, where the approximation (6) may be applied,
(3) mixed conductivity range, where Eq. (4) should be used.

As can be seen from Fig. 4 both plot 1 (electronic component of the electrical conductivity) and plot 2 (total electrical conductivity) differ in slopes of the linear dependencies in the n- or p- type regions and in curvatures in a mixed conductivity range.

The curvature of the dependency $y = \log\sigma = f[\log p(O_2)]$ is characterized by the radius of curvature, ρ:

$$\rho = \frac{(1 + y'^2)^{\frac{3}{2}}}{|y''|} \quad (7)$$

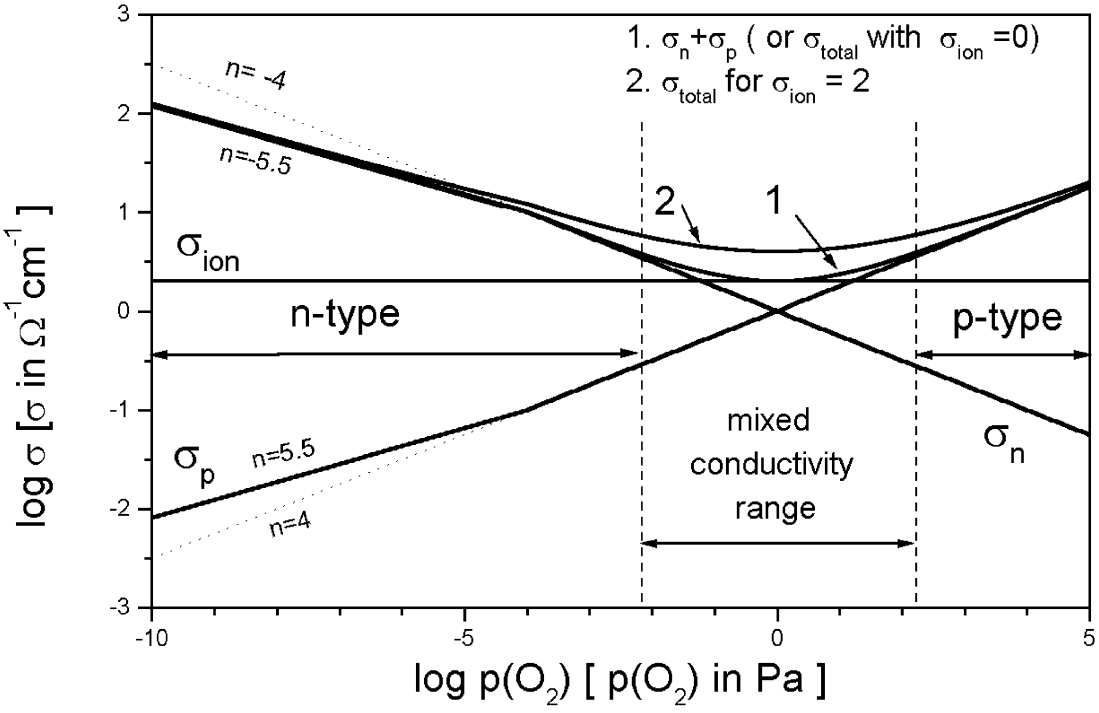

Fig. 4. Dependencies of σ_{tot}, σ_n and σ_p vs $p(O_2)$ for arbitrarily chosen parameters $\sigma_n^o = \sigma_p^o = 1$ and $\sigma_{ion} = 0$ (curve $\sigma_n + \sigma_p$) and $\sigma_{ion} = 2$ (curve σ_{total}).

where y' and y'' are first and second derivative log σ vs log $p(O_2)$, respectively. Applying (7) to (4) it is easily to deduce, that:

$$\rho_o = 8\sigma_{total,min}^2 = 8\left(\sigma_{el,min} + \sigma_{ion}\right)^2 \tag{8}$$

where ρ_o is the radius of the curvature at the point corresponding to the minimum value of σ_{total} and $\sigma_{el,min}$ is the minimum value of the electronic component of electrical conductivity. According to the relation (8) the radius of curvature of the plot 2 is four times higher than that of the plot 1.

The differences in slopes may be characterized by the reciprocal of the oxygen power dependence of the electrical conductivity, defined as:

$$m_\sigma = \left(\frac{\partial \log \sigma_{total}}{\partial \log p(O_2)}\right)_T^{-1} \tag{9}$$

Applying (9) to (4) we have:

$$m_\sigma = \frac{4\sigma_{total}}{\sigma_p - \sigma_n} \tag{10}$$

Fig. 5 illustrates the dependence m_σ on $p(O_2)$ for the same arbitrary chosen parameters as in Fig. 4. As can be seen, the parameter m corresponding to the electronic component of the electrical conductivity is very close to theoretical values $m_\sigma = -4$ and $m_\sigma = 4$ for n- and p-type, respectively. On the other hand the parameter m of the total electrical conductivity with not negligible value of the ionic component (σ_{ion}) differs substantially from $m_\sigma = -4$ and $m_\sigma = 4$ for n- and p- type, respectively.

Unfortunately, as it was mentioned above, the $p(O_2)$ ranges were TiO_2 exhibits 'pure' n- or p- type behavior is very narrow. Therefore, we resigned from commonly applied in literature[13–23] the approximations (5) and (6). Instead of this we applied curvilinear least squares method using the dependence (4). Applying a typical procedure based on minimalization of the squared sum:

$$\sum_{i=1}^{i=k}\left[\sigma_i - \sigma_n^o p_i^{-1} - \sigma_p^o p_i - \sigma_n^o\right]^2 \tag{11}$$

where $p = p(O_2)^{1/4}$, k is the number of experimental points, we get the following system of the linear equations in respect to σ_p^o, σ_n^o and σ_{ion}^o:

$$\begin{aligned}
&\sigma_p^o \sum_{i=1}^{i=k} p_1^2 + \sigma_n^o k + \sigma_{ion}^o \sum_{i=1}^{i=k} p_i = \sum_{i=1}^{i=k} \sigma_i p_i \\
&\sigma_p^o k + \sigma_n^o \sum_{i=1}^{i=k} p_i^{-2} + \sigma_{ion}^o \sum_{i=1}^{i=k} p_i^{-1} = \sum_{i=1}^{i=k} \sigma_i p_1^{-1} \\
&\sigma_p^o \sum_{i=1}^{i=k} p_i + \sigma_n^o \sum_{i=1}^{i=k} p_i^{-1} + \sigma_{ion}^o k = \sum_{i=1}^{i=k} \sigma_i
\end{aligned} \tag{12}$$

The obtained $\sigma_{ion}T$ values have been presented in Fig. 6 as a function of reciprocal temperature. The activation energies determined for the ionic component

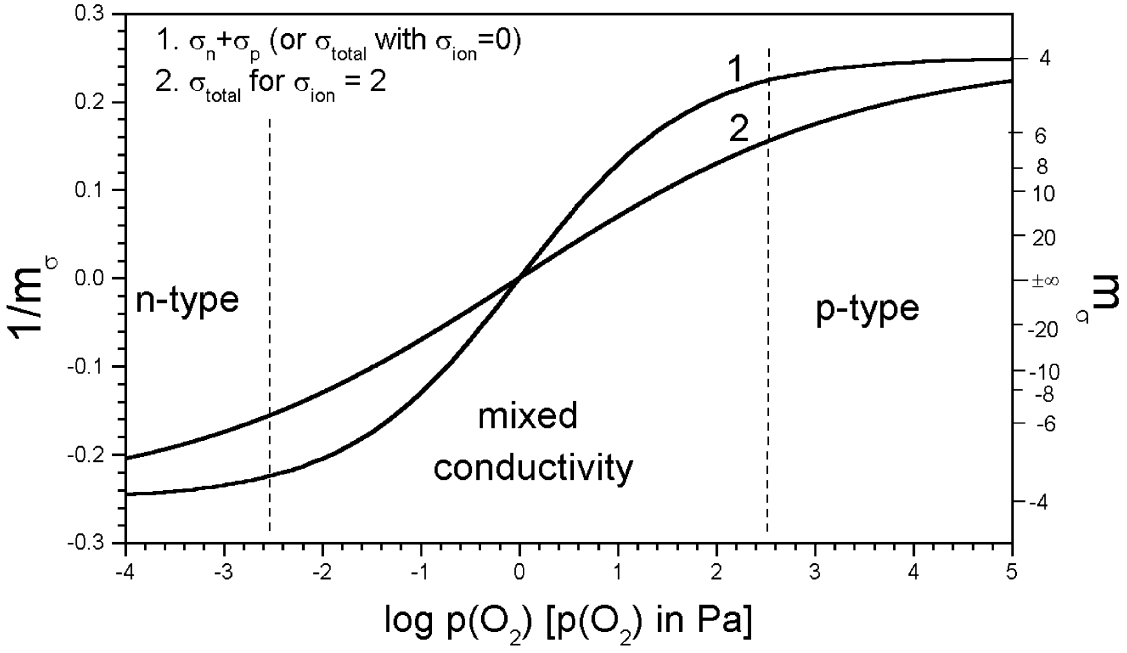

Fig. 5. Dependence of m_σ on p(O_2) for the same arbitrary chosen parameters as in Fig. 4.

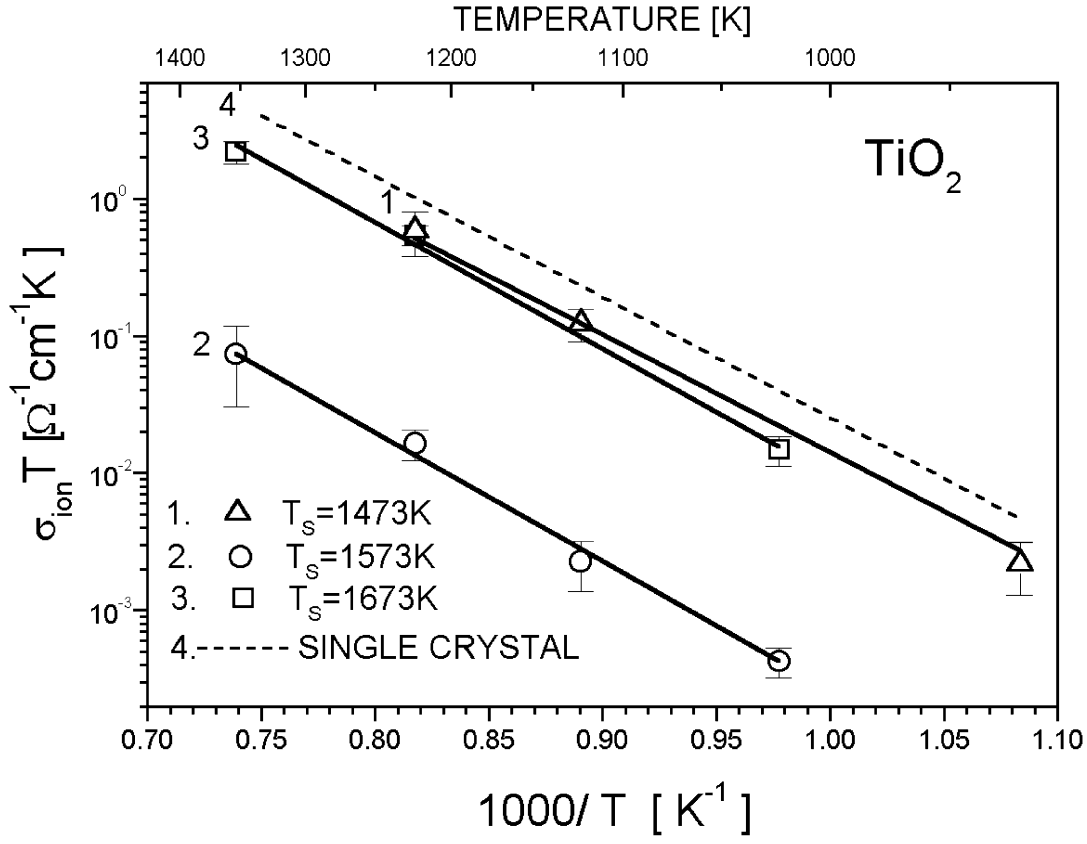

Fig. 6. Plot of (σ_{ion} T) as a function of reciprocal temperature for the ceramic samples (1–3) and the single crystal (4).

are similar, close to $E_{ion,act} = 1.78 \pm 0.08$ eV (Fig. 7). On the other hand, the absolute values of ionic conductivity differ substantially. Single crystals exhibit the highest ionic conductivity and polycrystalline TiO_2, sintered at 1300 °C (1573 K) has the lowest one. This result contradicts the findings reported in Ref. 11, which claims that ionic transport in TiO_2 is enhanced by the presence of grain boundaries.

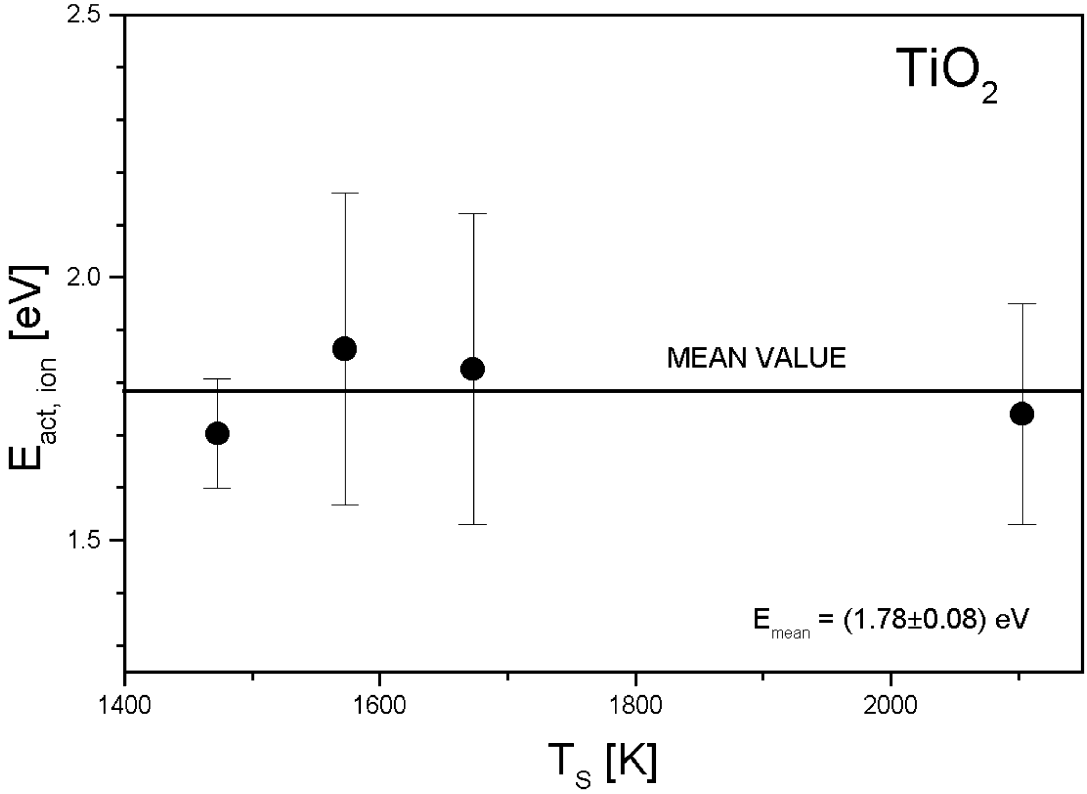

Fig. 7. Activation energy of the ionic electrical conductivity vs sintering temperature, T_S.

Fig. 8 illustrates the dependency of ionic transfer numbers, t_{ion}, on the temperature at which measurements were taken, T_M, at $p(O_2) = 2.5$ kPa. The ionic transfer number of the samples sintered at 1200 °C (1473 K) remains independent of temperature, at 1400 °C (1673 K) decreases with T_M, whereas for the sample sintered at 1300 °C (1573 K), the dependency is not monotone. Fig. 9 illustrates t_{ion} as a function $p(O_2)$ at $T_M = 1223$ K (950 °C). The observed maximum value of t_{ion} for the sample sintered at 1400 °C (1673 K) correspond to the same values $p(O_2)$ where minimum value of total electrical conductivity was observed (see Fig.). On the other hand as results from Figs. 1–2 there are no σ_{min} for the sample sintered at 1200 and 1300 °C (1473 and 1573 K) and, therefore, no maximum t_{ion} is observed in Fig. 9 in these cases.

4.2. Determination of diffusion coefficients

The ionic electrical conductivity component TiO_2 of is correlated to diffusion coefficients. According to Nerst–Einstein equation[27]:

$$\frac{\sigma^o_{ion}}{D_d} = \frac{c_d q_d^2}{kT} \tag{13}$$

where D_d (cm^2/s) is the diffusion coefficient of these ionic defects, which take part in the transport, and c_d and q_d are concentration and charge of these defects, expressed in cm^{-3} and C, respectively. D_d is related to the self diffusion coefficient, D_{self}, usually determined using the tracer diffusion method, or by the tracer diffusion coefficient, D_T:

$$D_{self} = D_d \frac{c_d}{c_a} \tag{14}$$

$$D_T = H_R D_{self} \tag{15}$$

where c_a (cm^{-3}) is the concentration of mobile atoms, H_R denotes the Haven ratio, which depends on crystal structure and on mechanism of diffusion (for interstitial diffusion mechanism $H_R = 1$). Inserting the Eq. (14) into Eq. (13) gives:

$$D_{self} = \frac{c_d q_d^2}{k}\left(\sigma^o_{ion} T\right) \tag{16}$$

The concentration of atoms, c_a, can be easily determined from the density of the material, d:

$$c_d = \alpha \frac{d}{M_{TiO_2}} N_A \tag{17}$$

where N_A is Avogadro's number ($N_A = 6.022*10^{23}$ mol^{-1}), M_{TiO_2} is the weight of TiO_2 ($M_{TiO_2} = 79.90$ g/

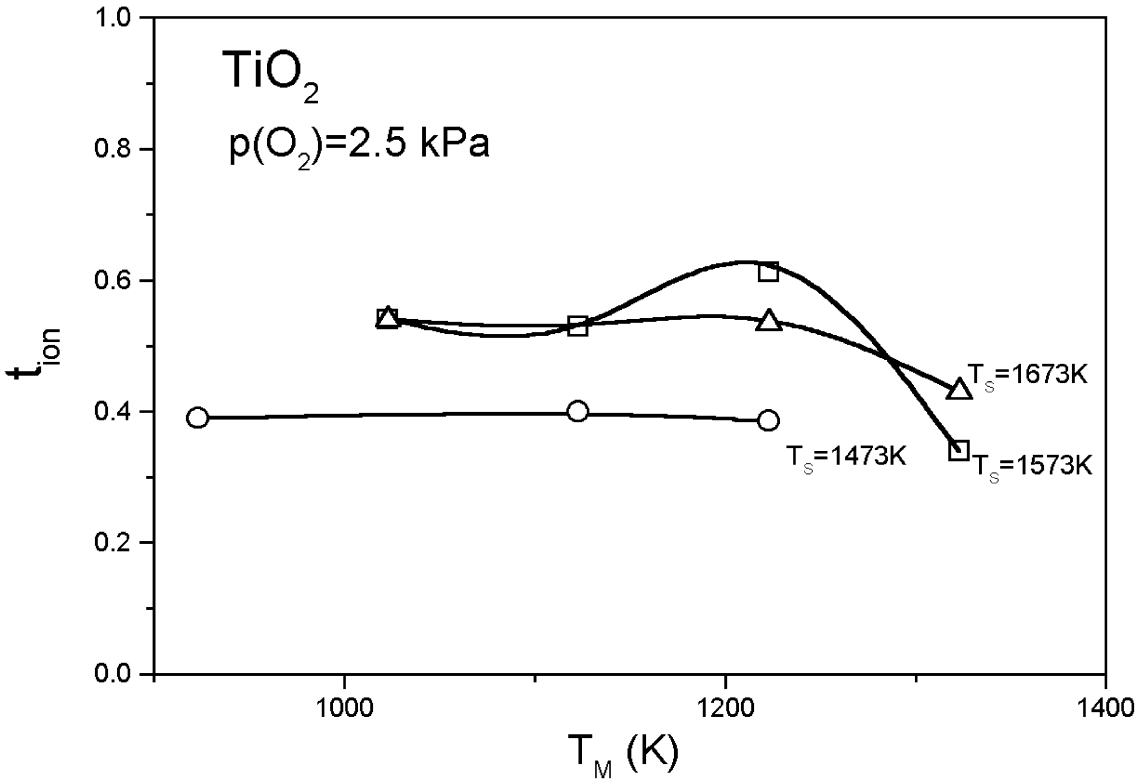

Fig. 8. Ionic transport numbers at $p(O_2) = 2.5$ kPa in TiO_2 sintered at 1200, 1300 and 1400 °C (1473, 1573 and 1673 K) as a function of temperature, T_M.

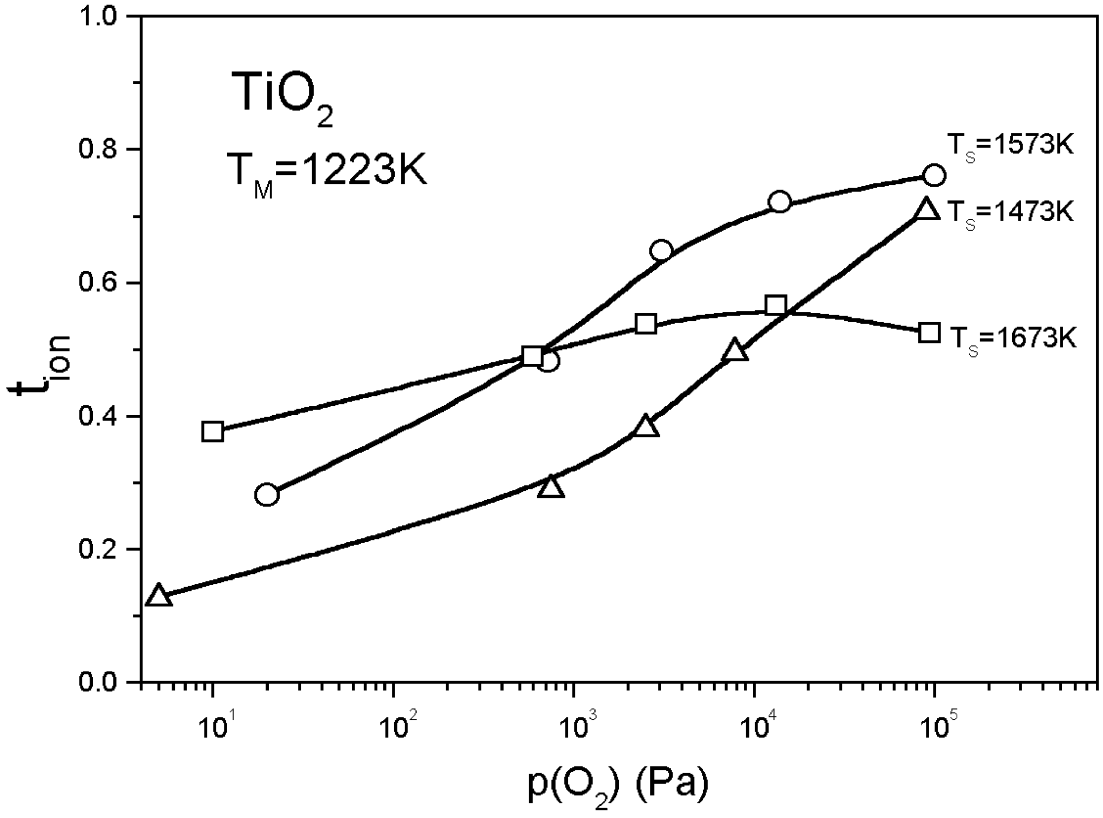

Fig. 9. Ionic transport numbers at 950 °C (1223 K) in TiO_2 sintered at 1200, 1300 and 1400 °C (1473, 1573 and 1673 K) as a function of oxygen partial pressure, $p(O_2)$.

mol) and α is equal to 1 or 2 if, respectively, titanium interstitial or oxygen vacancy are mobile defects. The density of TiO_2 is $d = 4.26$ g/cm^3.[28] So far, there are two competitive mechanisms described in the literature, explaining ionic conductivity of TiO_2 close to the n–p transition point. The first mechanism assumes transport of oxygen ions through the oxygen vacancies mechanism ($D_{self} = D_O$), the second-transport of titanium ions through interstitial mechanism ($D_{self} = D_{Ti}$). Taking into account the relationship (16) we estimated both coefficients. The results of our estimations are illustrated in Fig. 10[29–33] and 11[34–37] on the background of the available diffusion data. Our finding shows that titanium interstitial disorder predominates over oxygen vacancy models in the studied $p(O_2)$ and temperature ranges.

The comparison of absolute values of D_{Ti} (diffusion coefficient of TiO_2) for different samples shows that they are highest in the single crystal. It may suggest that the grain boundaries in ceramic materials have a retarding effect on the transport of titanium atoms. On the other hand, however, there is no simple correlation between D_{Ti} and sintering temperature, T_S.

4.3. Energy gap

The energy gap in studied materials was determined by the following methods:

(i) from optical measurements using the integrating sphere (which proved to be a very useful instrument for studies of powder and ceramic materials),
(ii) from the electrical conductivity measurements.

Optical measurements were used to determine the band gap energy E_g. Light scattering experiments provided a valuable aid in studying the surface roughness ceramics materials. Fig. 12 shows the diffused reflectance spectra of TiO_2 ceramics sintered at 1200, 1300 and 1400 °C (1473, 1573 and 1673 K). The data presented in Fig. 12 allow us to determine the band gap E_g. The exact positions of the absorption maxima are derived from the recorded first derivatives D_I of the spectra. The samples sintered at different temperatures show the same value of the forbidden gap E_g close to 3.0 eV.

Fig. 12 shows also the impact of sintering temperature, T_S, on diffused reflectance spectra. A much lower level of R_{Diff} for TiO_2 sintered at 1400 °C (1673 K) indicates a small contribution from surface roughness and volume scattering as compared with the TiO_2 sintered at 1473 K. The scattering is caused by the specific microstructure, large grains. Morphology of ceramics was found to be strongly affected by the temperature of sintering

The determined component of ionic conductivity also makes it possible to determine the electronic component

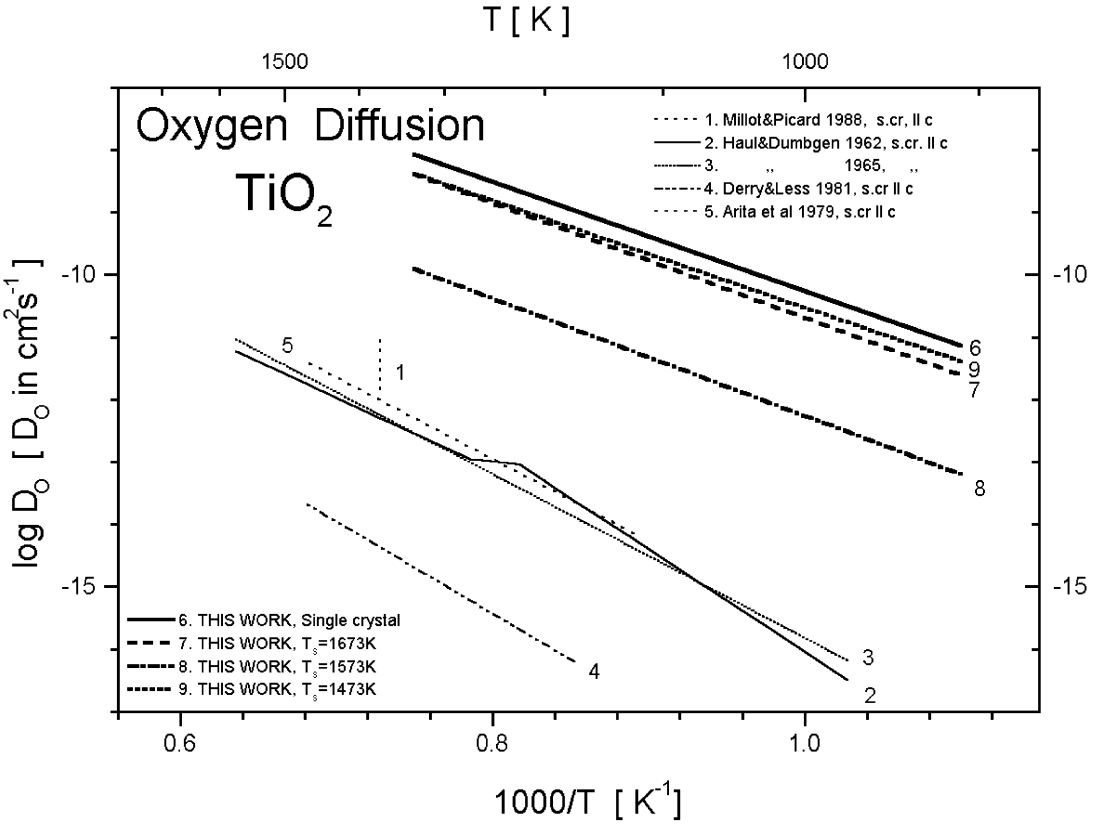

Fig. 10. Arrhenius plot of oxygen self diffusion coefficient in TiO_2.[29–33]

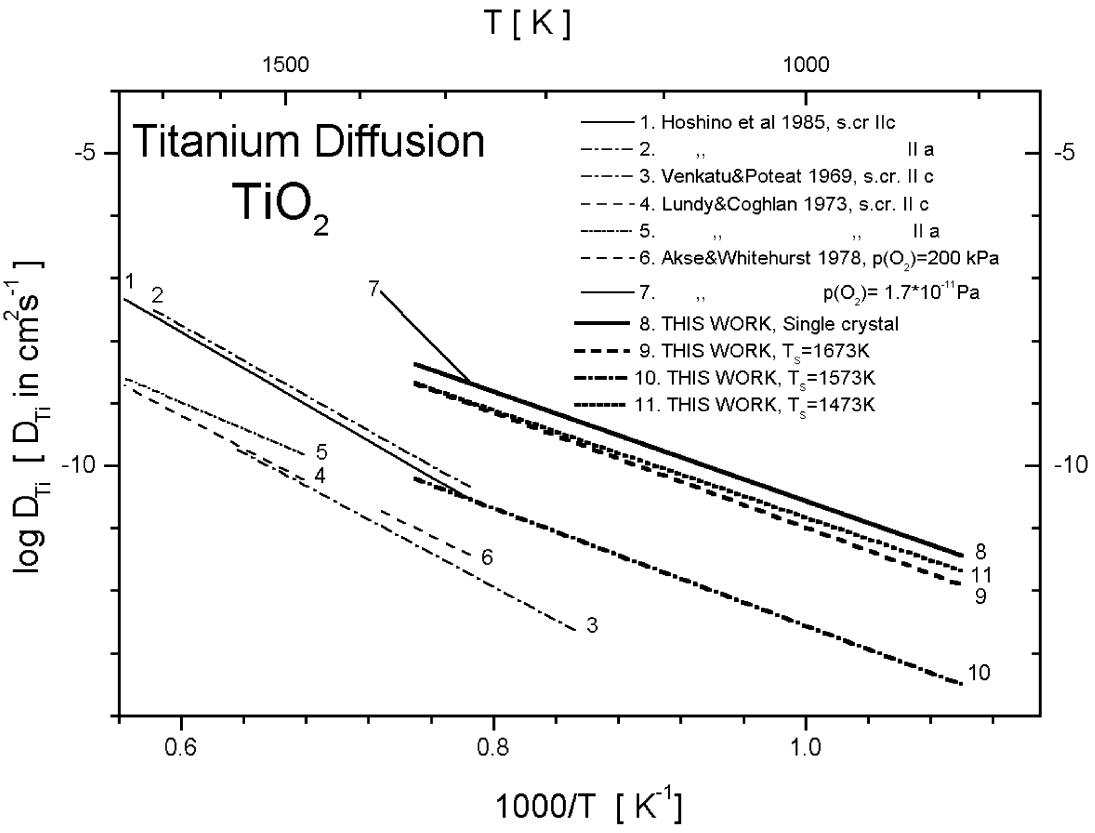

Fig. 11. Arrhenius plot of titanium self diffusion coefficient in TiO_2.[34–37]

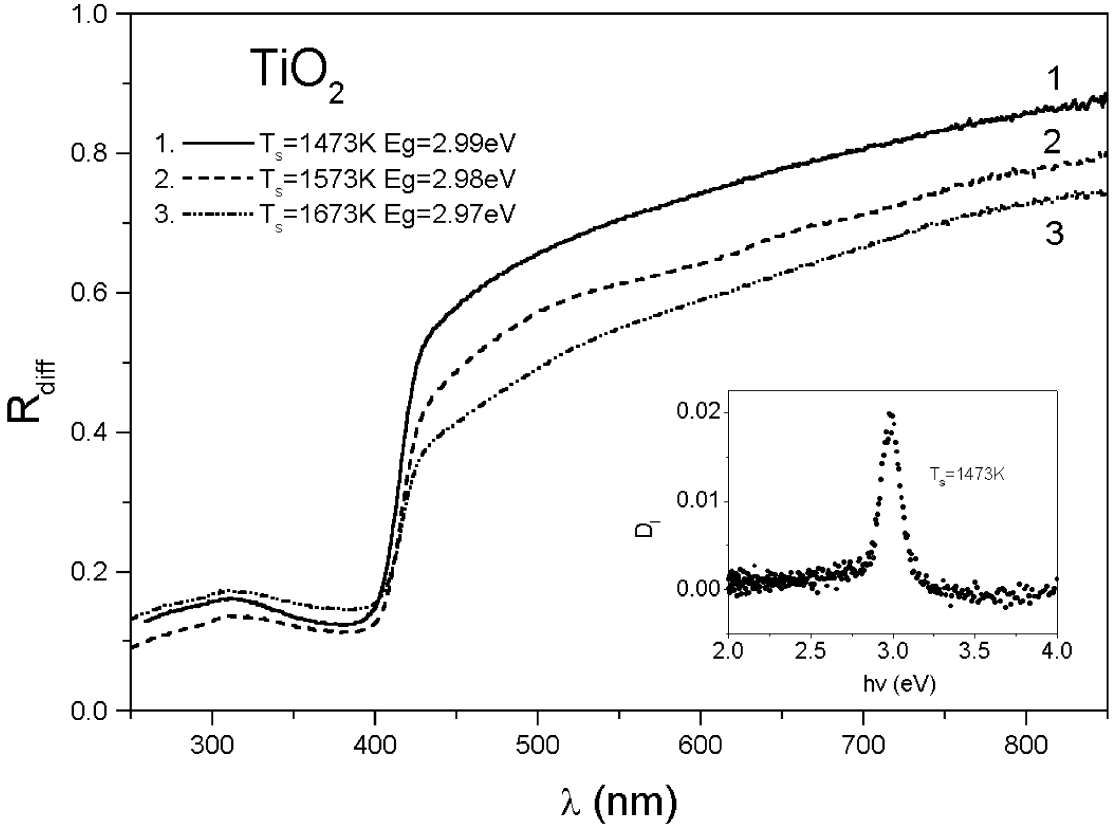

Fig. 12. Diffused reflectance spectra of TiO_2 ceramics sintered at 1200, 1300 and 1400 °C (1473, 1573 and 1673 K).

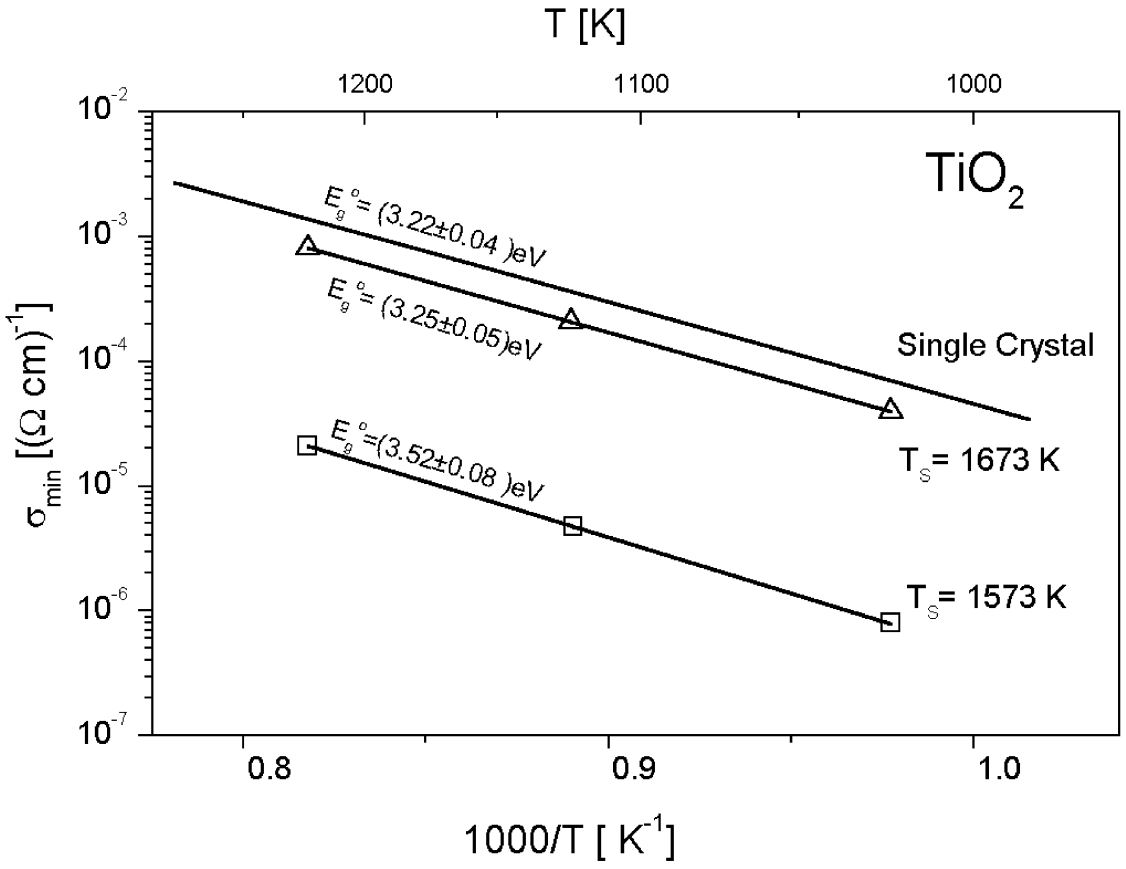

Fig. 13. Arrhenius plot of the minimum electrical conductivity (electronic component).

of conductivity (by subtracting ionic conductivity from total conductivity).

The minimum value of the electronic conductivity, σ_{min}, is the following function of temperature[38]:

$$\sigma_{min} = 2e(\mu_p \mu_n N_p N_n)^{1/2} \exp\left[-\frac{E_g}{kT}\right] \quad (18)$$

where: e is the elementary charge, μ the mobility (cm^2/Vs), N the density of states (cm^{-3}); p and n denote holes and electrons, respectively.

Fig. 13 illustrates the minimum value of the electronic conductivity, σ_{min}, as a function temperature T_M, in the Arrhenius coordinate system. The energy gap (determined from Fig. 13) exceeds E_g determined from optical studies by about 0.2–0.5 eV. There are two alternative explanations for the observed differences in 'optical' and 'electrical' E_g. The first is based on the temperature dependence of E_g. It is commonly assumed, that the changes with temperature of the energy gap may be expressed by the following relationship:

$$E_g = E_g^o - \beta T \quad (19)$$

Inserting Eq. (19) into Eq. (18) we can assume that the activation energy of the σ_{min} is equal to $E_g^o/2$ rather than $E_g/2$. On the other hand, the optical E_g corresponds to the room temperature. Table 1[9,39–41] illustrate the expected differences between 'electrical' (E_g^o) and optical E_g^{298K} energy gap. As can be deducted, the expected difference is about 0.2–0.4 eV. This value is close to that observed in this work.

The second explanation of the observed difference is temperature dependence of the product ($\mu_p \mu_n N_n N_p$) in the Eq. (18). For example, the difference may be interpreted as activation energy of the mobility of electronic carriers, which, in the case of the hopping mechanism is in the order of 0.1–0.2 eV[42].

On the other hand, the effect of sintering temperature on the electrical energy gap in TiO_2 was observed. This result cannot be explained by the effect of grain sizes on

Table 1
Temperature coefficient of the energy gap, β, and expected difference between electrical (E_g^o) and optical energy gap at room temperature (E_g^{298K})

β (eV/K)	$E_g^o - E_g^{298K}$ (eV)	Reference
$6.0*10^{-4}$	0.18	39
$8.9*10^{-4}$	0.27	40
$6.6*10^{-4}$	0.20	41
$13.3*10^{-4}$	0.40	9

energy gap. This finding agrees with the observations of other authors, reviewed in papers.[43,44] The energy gap of TiO_2 remains independent of grain size until grain size surpasses several nanometers. For smaller grain, the so-called quantum size effect is observed, which increases E_g.[43,44] According to microscopy analysis the grains of studied specimens considerably exceed this critical value. The observed effect of sintering temperature (T_S) on electrical energy gap is caused probably by the existence of grain boundaries and their impact on electrical properties.

5. Summary and conclusions

The discrepancy between the values of observed and theoretical dependencies of electrical conductivity on oxygen partial pressure was used to determine the ionic conductivity component at the $p(O_2)$ range close to the n–p transition point. The ionic conductivity was independent of oxygen activity. The activation energy of this ionic component is about 1.78 eV. Ionic transference numbers assume a value of ca. 0.7 at the p–n transition point. This parameter increases with $p(O_2)$, reaching a value of 0.8 at $p(O_2) = 0.1$ MPa for the sample sintered at 1300 °C (1573 K).

The verification of determined ionic conductivity components was done by the comparison estimated values of diffusion coefficients using the Nerst–Einstein relation and literature diffusion data. There is a good agreement between the two sets of compared data, assuming that titanium interstitial disorder prevails.

Electronic conductivity component (determined by subtracting the ionic component from the total electrical conductivity)was used to estimate the energy gap in TiO_2.

Acknowledgements

The financial support of Polish State Committee for Research (KBN), Grant No. 7 T08A 071 19 is gratefully acknowledged. Dr. Katarzyna Zakrzewska is acknowledged for her assistance during the experiments in the optical studies and her helpful discussion of the received results. We would like to thank Dr. Agata Rekas-Furolo and Mr. Jeff Furolo for reviewing this paper.

References

1. Yan, M. F. and Rhodes, W. W., Preparation and properties of TiO_2 varistors. *Appl. Phys. Lett*., 1986, **40**, 536–537.
2. Yan, M. F. and Rhodes, W. W., Varistor properties of (Nb,Ba)-doped TiO_2. In *Grain Boundaries in Semiconductors*, ed. H. J. Leamy, G. E. Pike and C. H. Seager. Elsevier Sci. Publ., NY, 1982, pp. 357–362.
3. Yang, S.-L. and Wu, J.-M., Effects of Nb_2O_5 in (Ba,Bi,Nb)-added TiO_2 ceramic varistors. *J. Mater. Res*., 1995, **10**, 345–352.
4. Yang, S.-L. and Wu, J.-M., Varied atmosphere compensation-exploring the roles of barium and bismuth in (Ba,Bi,Nb)-doped TiO_2 varistors. *J. Am. Ceram. Soc*., 1995, **76**, 2203–2208.
5. Yan, M. F. and Rhodes, W. W., Ultrahigh dielectric capacitance in TiO_2 ceramics. In *Additives and Interfaces in Electronic Ceramics*, ed. M. F. Yan and A. H. Heuer. Am. Ceram. Soc, Columbus, OH, 1983, pp. 226.
6. Rausch, N. and Burte, E. P., Thin TiO_2 films prepared by low pressure chemical vapor deposition. *J. Electrochem. Soc*., 1993, **140**, 145–149.
7. Farah, M. B., Lapicque, F. and Matlosz, M., Electrical characterization of the semiconducting properties of n-TiO_2. *J. Electrochem. Soc*., 1998, **145**, 3550–3556.
8. Bernasik, A., Radecka, M., Rekas, M. and Sloma, M., Electrical properties of Cr- and Nb-doped TiO_2, thin films. *Appl. Surf. Sci*., 1993, **65/66**, 240–245.
9. Nowotny, J., Radecka, M. and Rekas, M., Semiconducting properties of undoped TiO_2. *J. Phys. Chem. Solids*, 1997, **58**, 927–937.
10. Nowotny, J., Radecka, M., Rekas, M., Sugihara, S., Vence, E. R. and Weppner, W., Electronic and ionic conductivity of TiO_2 single crystal within n–p transition range. *Ceram. Int*., 1998, **24**, 571–577.
11. Maier, J., Schwitzgebel, G. and Hagenman, H. J., Electrochemical investigations of conductivity and chemical diffusion in pure and doped cubic $SrTiO_3$ and $BaTiO_3$. *J. Solid State. Chem*., 1985, **58**, 1–13.
12. Radecka, M. and Rekas, M., Effect of sintering temperature on n–p transition in TiO_2. *J. Am. Ceram. Soc* (in press).
13. Chang, E. K., Mehta, A., Smyth, D. M., Ionic transport numbers from equilibrium conductivities. In *Electro-Ceramics and Solid-State Ionics*, ed. H. L. Tuller, and D. M. Smyth. The Electrochemical Soc. 1988, pp. 35–45.
14. Bauerle, J. E., Electrical conduction in thoria and thoria-yttria as a function of oxygen pressure. *J. Chem. Phys*., 1966, **45**, 4162–4166.
15. Lasker, M. F. and Rapp, R. A., Mixed conduction in ThO_2 and ThO_2—Y_2O_3 solutions. *Z. Phys. Chem Neue Folge*, 1966, **49**, 198–221.
16. Iqbal, M. and Baker, E. H., Conductivity measurements on thoria–yttria solid solutions at high temperatures. *High Temp.-High Pressures*, 1973, **5**, 265–271.
17. Maiti, H. S. and Subbarao, E. C., Electrical conduction in CaO-doped thoria tlectrolytes. *J. Electrochem. Soc*., 1976, **123**, 1713–1718.
18. Patterson, J. W., Bogren, E. C. and Rapp, R. A., Mixed conduction in $Zr_{0.85}Ca_{0.15}O_{1.925}$ solid electrolyte. *J. Electrochem. Soc*., 1967;, **114**, 752–758.
19. Nasrallah, M. M. and Douglass, D. L., Ionic and electronic conductivity in Y_2O_3-doped monoclinic ZrO_2. *J. Electrochem. Soc*., 1974, **121**, 255–262.
20. Takahashi, T., Iwahara, H. and Esaka, T., High oxide ion conduction in sintered oxide of the system Bi_2O_3–M_2O_3. *J. Electrochem. Soc*., 1977;, **124**, 1563–1569.
21. Kilner, J. A., Barrow, P., Brook, R. J. and Norgett, M. J., Electrolytes for the high temperature fuel cell; experimental and theoretical studies of the perovskite $LaAlO_3$. *J. Power Sources*, 1978, **3**, 67–80.
22. Tuller, H. L. and Nowick, A. S., Doped ceria as a solid oxide electrolyte. *J. Electrochem. Soc*., 1975, **122**, 255–259.
23. Tuller, H. L., 1981. Defect structure and transport in oxygen excess cerium oxide-uranium oxide solid solutions. In *Transport in Nonstoichiometric Compounds*, ed. G. Simkowich, and V. S. Stubican, NATO ASI Ser., Plenum Press 1985, pp. 87–99.
24. Bridges, D. W., Baur, J. P. and Fassll, W. M. Jr., Effect of oxygen pressure on the oxidation rate of cobalt. *J. Electrochem. Soc*., 1956, **103**, 614–618.

25. Persels Constant, K., Mason, T. O., Rothman, S. J. and Routbort, J. L., Non-stoichiometry, electrical properties, and cation diffusion in highly non-stoichiometric $Co_{1-x}O$–I. Experimental. *J. Phys. Chem. Solids*, 1992, **53**, 405–411.
26. Sykora, G. P. and Mason, T. O., Defect studies above 1 atm oxygen: nickel monoxide and cobalt monoxide. *Adv. Ceram.*, 1987, **23**, 45–53.
27. Kofstad, P., *Nonstoichiometry, Diffusion, and Electrical Conductivity in Binary Metal Oxides*. Wiley Interscience, New York, 1972 (p. 86–87).
28. Weast, R.C., ed. *CRC Handbook of Chemistry and Physics*. CRC Press Inc. 1981, p. B138.
29. Millot, F. and Picard, C., Oxygen self-diffusion in non-stoichiometric rutile TiO_{2-x} at high temperature. *Solid State Ionics*, 1988, **28–30**, 1344–1348.
30. Haul, R. and Dümbgen, G., Untersuchung der sauerstoffbeweglichkeit in titandioxid, quarz und quarzglas mit hilfe des heterogenen isotopenaut-stausches. *Z. Elektrochemie*, 1962, **66**, 636–640.
31. Haul, R. and Dümbgen, G., Sauerstoff-selbstdiffusion in rutilkristallen. *J. Phys. Chem. Solids*, 1965, **26**, 1–10.
32. Derry, D. J., Less, D. G. and Calvert, J. M., A study of oxygen self-diffusion in the c-direction of rutile using a nuclear technique. *J. Phys. Chem. Solids*, 1981, **42**, 57–64.
33. Arita, M., Hosoya, M., Kobayashi, M. and Someno, M., Depth profile measurement by secondary ion mass spectroscopy for determining the tracer diffusivity of oxygen in rutile. *J. Am. Ceram. Soc.*, 1979, **62**, 443–447.
34. Hoshino, K., Peterson, N. L. and Wiley, C. L., Diffusion and point defects in TiO_{2-x}. *J. Phys. Chem. Solids*, 1985, **46**, 1397–1411.
35. Venkatu, D. A. and Poteat, L. E., Diffusion of titanium in single crystal rutile. *Mater. Sci. Eng.*, 1969, **5**, 258–262.
36. Lundy, T. S. and Coghlan, W. A., Cation self diffusion in rutile. *J. Phys. Coll.*, 1973, **C9**, 299–302.
37. Akse, J. R. and Whitehurst, H. B., Diffusion of titanium in slightly reduced rutile. *J. Phys. Chem. Solids*, 1978, **39**, 457–465.
38. Nowotny, J. and Rekas, M., Defect structure, electrical properties and transport in barium titanate. III. Electrical conductivity, thermopower and transport in single crystalline $BaTiO_3$. *Ceram. Int.*, 1994, **20**, 225–235.
39. Yahia, J., Dependence of the electrical conductivity and thermoelectric power of pure and aluminum-doped rutile om equilibrium oxygen pressure and temperature. *Phys. Rev.*, 1963, **130**, 1711–1719.
40. Bube, R. H., *Photoconductivity of Solids*. Wiley, New York, 1960 p. 237).
41. Baumard, J. F. and Tani, E., Thermoelectric power in reduced pure and Nb-doped TiO_2 rutile at high temperature. *Phys. Status Solidi(a)*, 1977, **39**, 373–382.
42. Austin, I. G. and Mott, N. F., Polarons in crystalline and non-crystalline materials. *Adv. Phys.*, 1969, **20**, 225–235.
43. Henglein, A., Small-particle research: physicochemical properties of extremely small colloidal metal and semiconductor particles. *Chem. Rev.*, 1989, **89**, 1861–1873.
44. Hagfeldt, A. and Grätzel, M., Light-induced redox reactions in nanocrystalline systems. *Chem. Rev.*, 1995, **95**, 49–68.